IEEE Access
Multidisciplinary | Rapid Review | Open Access Journal

IEEE GEOSCIENCE AND REMOTE SENSING SOCIETY SECTION

Received 31 October 2023, accepted 30 November 2023, date of publication 18 December 2023,
date of current version 21 December 2023.

Digital Object Identifier 10.1109/ACCESS.2023.3343916

RESEARCH ARTICLE

Coded Pulse Stream LiDAR Based on Optical Orthogonal Frequency-Division Multiple Access

GUNZUNG KIM[1], (Member, IEEE), IMRAN ASHRAF[2], JEONGSOOK EOM[3], AND YONGWAN PARK[2], (Member, IEEE)

[1]Institute of Information and Communication, Yeungnam University, Gyeongsan-si, Gyeongsangbuk-do 38541, Republic of Korea
[2]Department of Information and Communication Engineering, Yeungnam University, Gyeongsan-si, Gyeongsangbuk-do 38541, Republic of Korea
[3]Department of Multimedia and Communication Engineering, Yeungnam University, Gyeongsan-si, Gyeongsangbuk-do 38541, Republic of Korea

Corresponding author: Yongwan Park (ywpark@yu.ac.kr)

This work was supported by the Basic Science Research Program through the National Research Foundation of Korea (NRF) funded by the Ministry of Education under Grant NRF-2021R1A2B5B02086773, Grant NRF-2021R1A6A1A03039493, and Grant NRF-2022R1I1A1A01070998.

ABSTRACT In future mobility, robust obstacle detection is imperative for autonomous vehicles, fostering a reliance on vision-based data and the emergence of light detection and ranging (LiDAR) as a pivotal sensor. Despite challenges of cost and novelty, LiDAR's unique capabilities find favor among automakers, except Tesla. Offering 3D imaging with superior resolution than radar, LiDAR holds potential significance as a perception sensor for safe and efficient transportation. Its 3D distance measurement using laser pulses and waveform analysis is vital for obstacle detection in autonomous vehicles. Techniques like scanning and flash LiDAR optimize point cloud acquisition, albeit with challenges in balancing resolution and frame rates. Because LiDAR measures the distance to an object using the time-of-flight, the idle listening time required to detect reflected waves increases in proportion to the maximum distance. Both, lateral angular resolution and frame rates are dependent on this idle listening time. Lateral angular resolution impacts LiDAR's ability to detect objects. This study proposes an optical orthogonal frequency-division multiple access (OFDMA) LiDAR with a coded pulse technique to enhance the detection accuracy of objects. Simulation results demonstrate that the proposed OFDMA LiDAR overcoming false positives and mutual interference through pulse stream LiDARs and strategic approaches is crucial in LiDAR's integration into future mobility systems.

INDEX TERMS Autonomous vehicles, LiDAR, optical communication, optical OFDMA, time-of-flight, discrete Hartley transform.

I. INTRODUCTION

Future mobility is foreseen to include a diverse variety of vehicles including airborne or flying vehicles, similar to today's ground vehicles. The mobility solutions must be able to detect and react to obstacles in their environment to ensure safe and efficient transportation [1], [2], [3], [4]. Similar to how humans rely on visual cues for navigation, vision-based data plays a critical role in identifying and detecting obstacles in the path of mobility systems. Light detection and ranging (LiDAR) is the most widely used sensor available for visual sensing. Compared to cameras and radars, LiDAR is a relatively new and expensive technology, which has limited its widespread use. However, LiDAR has unique features that distinguish it from other sensors. LiDAR is expected to play a critical role in the future of mobility, especially in autonomous vehicles. Except for Tesla, most automakers have already adopted LiDAR to enhance autonomous driving capabilities.

LiDAR provides complete spatial understanding by creating 3D images of the environment. A key advantage of LiDAR over radar is its relatively high lateral angular resolution, which improves object detection and localization accuracy [5]. However, LiDAR is limited in frame rates and may provide comparatively lower frame rates than other perception sensors. LiDAR requires further performance

The associate editor coordinating the review of this manuscript and approving it for publication was Stefania Bonafoni.

improvements due to a trade-off between lateral angular resolution and frame rate. As LiDAR technology advances, lateral angular resolution, and frame rate challenges must be addressed simultaneously. Despite its potential for future transportation, the high cost of LiDAR is a big challenge that has limited its wide application in mobility. In addition, shock-prone and vibration-prone optical components for LiDAR are another big challenge. Once these challenges are overcome, LiDAR can fulfill its potential as an essential perception sensor for future mobility, leading to an era of safe and efficient transportation systems.

- This study proposes an optical orthogonal frequency-division multiple access (OOFDMA) LiDAR with a coded pulse technique for object detection. We proposed an optimized flip-OFDM based on discrete Hartley transform (DHT) for OOFDMA LiDAR.
- The proposed LiDAR measures long-distance with high lateral resolution and high frame rate without loss of accuracy and precision.
- The proposed LiDAR does not interfere with each other, even when more than one unit is operating simultaneously, allowing cooperative operation.
- Simulations are performed to validate the performance of the prototype of the proposed OOFDMA LiDAR. For this purpose, its performance is compared with pulsed LiDAR, sequential firing LiDAR, unipolar concurrent firing LiDAR, and bipolar concurrent firing LiDAR.

The remaining paper is organized as follows. Limitations of LiDAR are presented in Section II. Section III presents the architecture and working mechanism of the proposed LiDAR. Section IV describes the simulation setup, results, and analysis of the results. Finally, Section V presents the conclusion and future works.

II. LIMITATIONS OF LiDAR WITH SINGLE PULSE OR CODED PULSE STREAM

A. BASIC LiDAR OPERATION

LiDAR is characterized by its ability to measure distance in three dimensions. When measuring the distance of an object, LiDAR systems emit laser pulses and capture their reflections, then calculate the distance based on the time taken for the laser to complete a round-trip [4], [6]. Each LiDAR system can measure a maximum distance, which depends on factors such as the laser's emission characteristics and wavelength, the receiver's sensitivity, and the employed signal processing technique. LiDAR systems allocate sufficient time for the transmitted laser to travel the maximum distance at the speed of light and receive the reflected wave.

Due to the laser's constant speed, LiDAR systems implement various techniques to measure as many points as possible within a specific period. One technique that LiDAR systems use is the scanning LiDAR approach, in which each laser pulse is directed to an individual point, one at a time [7]. The distance is measured after the reflected wave is intercepted before the LiDAR moves towards the following point, with a slightly different angle. However, this approach can measure only one point at a time, resulting in significant time consumption when measuring many points. Nevertheless, the advantage of this approach lies in the concentrated laser power, which allows measurements of greater distances. On the other hand, the flash LiDAR approach can quickly measure numerous points by projecting a laser pulse to the targeted area like a camera flashlight and receiving the corresponding reflected waves [6]. However, the flash LiDAR method has a disadvantage in terms of distance. The laser's power is spread over a broader area which reduces the measurement distance.

Certain scanning LiDARs employ simultaneous laser emission across multiple points to mitigate this limitation, reducing the desired area's measurement time. Velodyne's Alpha Prime is an outstanding LiDAR system with 128 laser diodes, each designating a single of 128 points [7]. These lasers are arranged as groups of eight lasers and are capable of simultaneous transmission. Each group transmits every 2.665 µs, following 16 transmit sequences, to measure the distance. Despite its versatility, Alpha Prime's measurement process takes at least 50 milliseconds to measure the same location after covering all areas, making it unsuitable for detecting fast-moving objects.

B. LATERAL ANGULAR RESOLUTION

The lateral angular resolution of a LiDAR system is crucial in determining the frame rate for repeated measurements of the same location [3], [4]. The scanning LiDAR completes the measurement of one angle. It changes the angle slightly and then measures the next angle. When measuring a given area, the angle of movement becomes smaller in proportion to the resolution, increasing the number of measurements. Consequently, measurement time increases proportionally, and the frame rate decreases. Utilizing a high lateral angular resolution with a low frame rate is advantageous for precisely measuring stationary objects [6], [8], [9]. Using a high frame rate with a low lateral angular resolution is more beneficial for objects in high-speed motion. The lateral angular resolution also determines the minimum size of accurately measurable objects. A scanning LiDAR emits laser pulses that rotate around a center regularly based on the lateral angular resolution. The LiDAR determines the position of an object by analyzing the reflected pulse. The distance between the LiDAR and the measured object, multiplied by the lateral angular spacing, determines the object's measurement interval. If the object's size exceeds the measurement interval, at least one laser pulse will reflect, enabling the measurement of its distance and identification of its presence. If the object's size is smaller than the measurement interval, at most, only one laser pulse can reflect from the object. The object's distance cannot be measured without laser pulse reflection, and its presence remains unknown. The maximum measurement interval is determined by the minimum size of the object recognized at the farthest measurement distance, which establishes the

rotation angle and lateral angular resolution. As it affects the minimum size and maximum speed of accurately measurable objects, selecting an optimized lateral angular resolution for specific applications is the responsibility of scanning LiDAR manufacturers.

LiDAR systems that use a single laser pulse are subject to similar limitations, regardless of the chosen transmission method. Researchers have explored coded pulses using randomized or optical code division multiple access (OCDMA) techniques to overcome these limitations [9], [10], [11]. This method transmits a coded laser pulse stream with unique codes to distinguish each measurement location. Subsequently, the system receives the reflected laser pulse stream from the object and decodes it to identify the corresponding measurement points. This process enables accurate calculation of travel time and distance. In the domain of radio frequency (RF), the CDMA method allows for the use of "+1", "0", and "−1" in the code. This method utilizes the properties of "+1" and "−1" to effectively cancel each other out, resulting in concise and efficient symbols. On the other hand, OCDMA is limited to "+1" and "0". As a result, a method is implemented to distinguish between "+1" and "0" based on the relative position and number of laser pulses [12]. This results in producing symbols and time bins that are less efficient and longer. Code length significantly impacts the stream of coded pulses the LiDAR transmits to a given point and the time required to transmit the pulses, resulting in longer times for measurement. LiDAR systems using single pulse or coded pulse streams take a long time because they must divide many locations into sequences for successive measurements or transmit many pulses. In improving LiDAR lateral angular resolution, the best approach is to decrease the dwell time by reducing the number of time bins and the encoded pulse stream length.

Pulse streams consist of multiple, irregularly spaced pulses. In the case of stationary objects, all laser pulses within a pulse stream are reflected from the same point, resulting in the same time of flight and distance measurements. However, for moving objects, the laser pulses within a pulse stream will be reflected from different points depending on the direction of the object, resulting in a different time of flight and distance measurement for each pulse. It is essential to transmit all laser pulses within the pulse stream in the shortest possible time to ensure accurate and precise distance measurement of a moving object. OCDMA code is critical to both coded pulse length and maximum measurable distance. Due to the potential health hazards of lasers, regulations limit the maximum permissible exposure (MPE) based on the number of laser pulses per second. Increasing the number of laser pulses in the pulse stream reduces the power per pulse transmitted by the LiDAR, consequently reducing the maximum distance that can be measured. Reducing the laser pulses per time bin increases the maximum measurement distance.

C. MEASUREMENT OF DISTANCE AND VELOCITY

The distance measuring algorithms employed in LiDAR systems rely on analyzing the waveform of the received reflected waves from the emitted pulses [6]. There are several types of methods including intensity-based, peak-intensity, and methods that consider both the width and height of the reflected waves. As the laser pulse passes through the medium toward the target object, it encounters particles and contaminants such as dust and moisture. Consequently, the laser pulse intensity decreases, and its waveform changes. When the laser pulse hits the surface of the target, part of the pulse is absorbed, the part passes through, and the rest is reflected. This results in a significant reduction in intensity and deformation of the waveform. The reflected energy distribution follows a hemisphere, leading to relatively low energy return to the LiDAR, even at high reflectivities. As the reflected laser pulse travels to the LiDAR receiver, further interactions with particles and contaminants affect its intensity and waveform. These interactions introduce additional variations from the original transmitted waveform. These waveform irregularities can significantly impact distance measurement methods that rely on the characteristics of the laser pulse, leading to a decrease in accuracy and precision. Pulse deformation can introduce significant errors when using a single-pulse LiDAR for distance measurement. Although the same site may be surveyed many times with a single pulse LiDAR, variations in the waveform caused by environmental conditions may result in slight variations in the range. On the other hand, pulse stream LiDARs overcome these limitations by using multiple pulses to measure and compute distance, thereby significantly improving accuracy and precision by the central limit theorem (CLT).

Single pulse methods set a minimum threshold for the reflected pulse to distinguish it from background noise to reduce false positives [6]. Lowering this threshold allows longer-range measurements but increases the probability of taking noise for a reflected pulse from an object. LiDAR systems choose to minimize false positives over maximizing measurement distance by carefully setting the threshold for the reflected pulse to be clearly distinguished from noise [4]. Pulse-stream LiDAR systems mitigate false positives by combining multiple pulses, allowing a reflected pulse threshold to match noise levels closely. A reflected pulse stream is only detected if all the pulses match the transmitted pulse stream. This pulse stream approach allows noise signals similar in magnitude to the reflected pulse to be ignored if they do not match the pulse pattern, thus eliminating the possibility of false positives. This feature reduces the reflected pulse threshold and increases the sensing range.

Some LiDAR uses frequency-modulated continuous wave (FMCW) technology to measure the distance and speed simultaneously from the Doppler shift of the moving target [6]. While pulsed LiDAR specializes in measuring

distance only using a single pulse, this approach is rarely used due to the challenges associated with detecting wavelength changes in the laser pulse to measure speed. This single-pulse approach can lead to significant errors. In contrast, the OCDMA method is more suitable for measuring the speed of an object because it uses multiple pulses instead of a single pulse. However, the pulses within the OCDMA pulse stream are sparsely spread, which makes it difficult to accurately detect the Doppler shift of the reflected waves because these pulses occur irregularly throughout the pulse stream. With consecutive pulse transmission, changes in wavelength can be accurately detected, allowing for more accurate measurements of an object's speed.

D. MUTUAL INTERFERENCE

In the perception sensor, cameras act as passive sensors without a signal source. Passive sensing allows multiple cameras to operate simultaneously without interfering with each other. In poor lighting situations, where cameras use a flash to light up the surroundings, the use of a flash from one camera affects the entire area of its range. Flashing can lead to errors in the captured images if another camera in the same area receives the light emitted by the flash. Radar and LiDAR are active sensors that rely on their signal source to measure distance. Radar and LiDAR determine distance through the transmission of a signal and the time needed to reflect and reach the receiver. When several radars or LiDARs operate simultaneously, they may encounter signals transmitted by other radars or LiDARs directly or after bouncing off objects. When these sensors receive a signal similar to the one transmitted, they cannot distinguish whether it is coming from the same sensor or another sensor. As a result, all the received data is processed as if it came from the same sensor, and time and distance are measured. Thus, wherever distance is calculated, an object is assumed to exist, including both real and false objects created by interfering with each other [13], [14]. The objects falsely detected due to mutual interference are known as ghost targets. In radar and LiDAR systems, this phenomenon is known as mutual interference. Mutual interference is more likely to occur when a received signal is much weaker than a transmitted signal, especially in systems that detect weak signals over long ranges. Radar systems have the advantage of precise frequency tuning, making it possible for different radars to operate on different frequencies to mitigate mutual interference. Furthermore, radar systems are available with different frequency bands to suit different applications, and technological advances have increased the number of available frequency bands.

The wavelength of the laser generated by the laser diode used in LiDAR systems is determined by its material properties, making it impossible to tune the wavelength for transmission. Consequently, LiDARs using the same laser diode share the same laser wavelength, increasing the risk of interference between multiple LiDARs operating simultaneously. In addition, the wavelength of the laser affects human vision. LiDAR emissions are visible to the naked eye and may cause health problems. The ultraviolet band is also not ideal for mobile LiDAR, as emissions from this band can cause severe adverse effects and health risks. This limits the bands that can be used as signal sources for future mobile LiDARs to infrared bands, which do not pose a significant health risk. Compared to other sensors, LiDAR is highly susceptible to mutual interference. As LiDAR technology becomes more widespread in future mobility, the probability of mutual interference in such scenarios is expected to increase. Therefore, mitigation strategies are needed to address the issue of mutual interference in future mobility systems incorporating LiDARs. The use of multiple LiDARs at the same time becomes a viable option when a single LiDAR system is unable to provide sufficient information for safe driving.

III. OOFDMA-BASED LiDAR

A. DESIGN CONCEPT

This study presents a new LiDAR that utilizes optical orthogonal frequency division multiple access (OOFDMA) to generate a laser pulse stream, as illustrated in Figure 1. The proposed LiDAR employs pulse stream generated by special coding techniques, rather than a single pulse, to ensure that only the pulses it sends are distinguishable, eliminating mutual interference [9], [10], [11], [14], [15], [16], [17]. However, coding techniques in optics can only use the presence of light, limiting them to represent only zeros (''0''s) and positives (''+1''s), unlike RF which can represent negative numbers (''−1''s). To represent a single bit in optics, a very long pulse stream is required which results in a long time to transmit the pulse stream [12], [18]. This LiDAR uses a pulse stream coded with OOFDMA to encode information into a very short length and then carried on multiple wavelengths from dense wavelength-division multiple-access (DWDMA) recommendations. Alternative access approaches for visible light communication (VLC) encompass time division multiple access (TDMA), frequency division multiple access (FDMA), and CDMA [19], [20]. FDMA mandates a guard band, resulting in lower spectral efficiency than OFDMA, allowing for overlapping adjacent bands. Although TDMA is orthogonal, it is less power-efficient than non-orthogonal alternatives like CDMA, which has been extensively investigated in radio frequency and suggested for VLC channels. We chosed OFDMA as it can accommodate more users without causing interference and is effective in scenarios involving VLC. OOFDMA is a computationally intensive coding technique that produces a very short pulse stream, making it well-suited for LiDAR [12], [21], and then the pulse streams are directed toward the target direction. 128 laser diodes and external optical modulators (EOMs) with varying wavelengths are utilized to produce transmit signals with different wavelengths. For the optical steering mechanism, we adopted Risley prisms that offer benefits for beam steering compared to other systems. These benefits comprise compactness, reduced sensitivity to vibration,

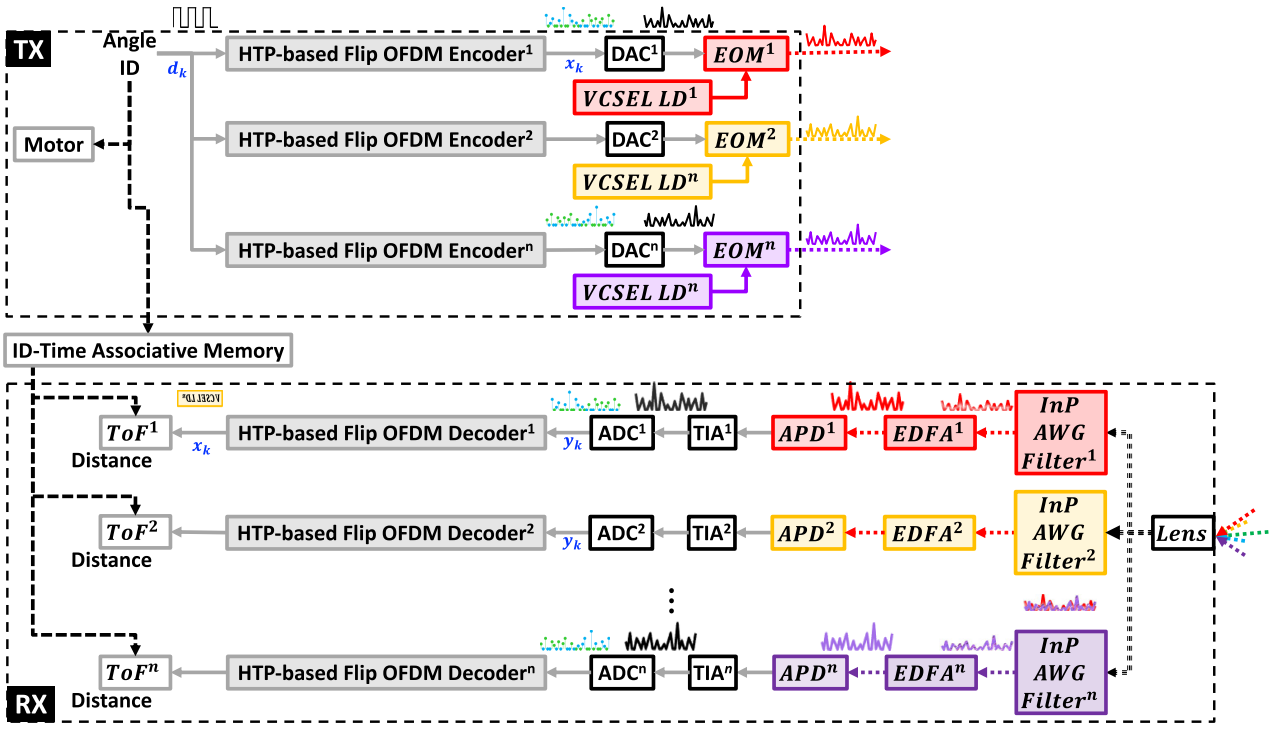

FIGURE 1. Overall operation of transmitter and receiver.

robustness, independent rotational axes, and low moment of inertia speed [22].

B. WORKING PRINCIPLE

The proposed LiDAR employs various techniques to ensure accurate measurements while minimizing mutual interference between laser signals. One of these techniques involves using the device and encrypted identifiers to specify the transmission direction of the corresponding laser signal. By modulating the encrypted identifiers through OOFDMA modulation, multiple laser signals with different wavelengths can be generated and transmitted simultaneously in various target directions. This approach effectively prevents mutual interference between laser signals transmitted simultaneously or by other LiDARs. In addition, LiDAR utilizes a pulse stream generated by optical coding techniques to ensure that only the pulses it sends are distinguishable, thereby eliminating mutual interference. Changing the transmission direction of the laser signal, irrespective of whether a reflected signal is received or not, also reduces the latency for distance measurement.

The transmission data is generated using flip-OFDM based on DHT and separated into each subchannel [12], [21], [23], [24], as shown in Figure 2 and Figure 3. Figure 2 shows the process of creating a transmission signal using OOFDMA, and Figure 3 shows the process of receiving a reflected wave in reverse order. The laser diodes are rotated concerning the direction of laser pulse emission and measurement interval of LiDAR scanning. The linear movement of the diodes is controlled to ensure appropriate measurement density [25], [26]. Once the received subchannels are combined, OOFDMA is used to restore the data. Apart from measuring the distance of objects, the proposed LiDAR also measures signal strength and pulse width. Several signal processing techniques, including optical aberration correction, are utilized to enhance the accuracy and reliability of the measurements [21].

Most OOFDMA approaches employ inverse discrete Fourier transform (IDFT) and DFT for multiplexing/ demultiplexing of the subchannels. As shown in Figures 2 and 3, this study employs DHT and inverse DHT (IDHT) for multiplexing and demultiplexing of the subchannels, provided that the input alphabets are drawn from real constellations such as M-ary pulse amplitude modulation (PAM). The kernel for both DHT and IDHT is identical, so the same algorithm can carry out both processes. Unlike conventional approaches that require Hermitian symmetric (HS) in the frequency domain (FD) to obtain a real-valued time domain (TD) signal, the proposed method generates a real-valued output for DHT/IDHT when a real-valued input is provided. By controlling the power of the emitted laser, it is possible to measure at different distances. The distance is measured by utilizing the flight time of the signal, while the object's relative speed can be determined by measuring the Doppler shift of the subchannel. OOFDMA suffers from a high peak-to-average power ratio (PAPR) due to the constructive addition of subchannels, which can be a significant limitation for intensity modulation-direction detection (IM-DD) systems with class-1 lasers that have a maximum optical output power less than the accessible

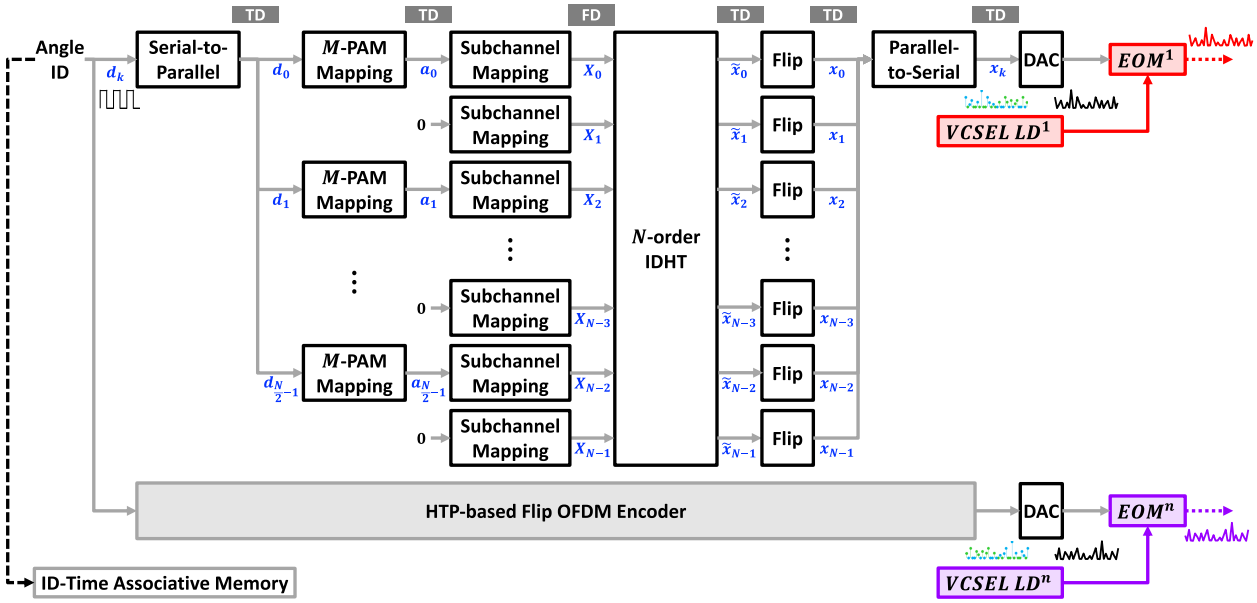

FIGURE 2. Signal processing sequences of the DHT-based flip-OOFDMA encoder at each transmission carrier.

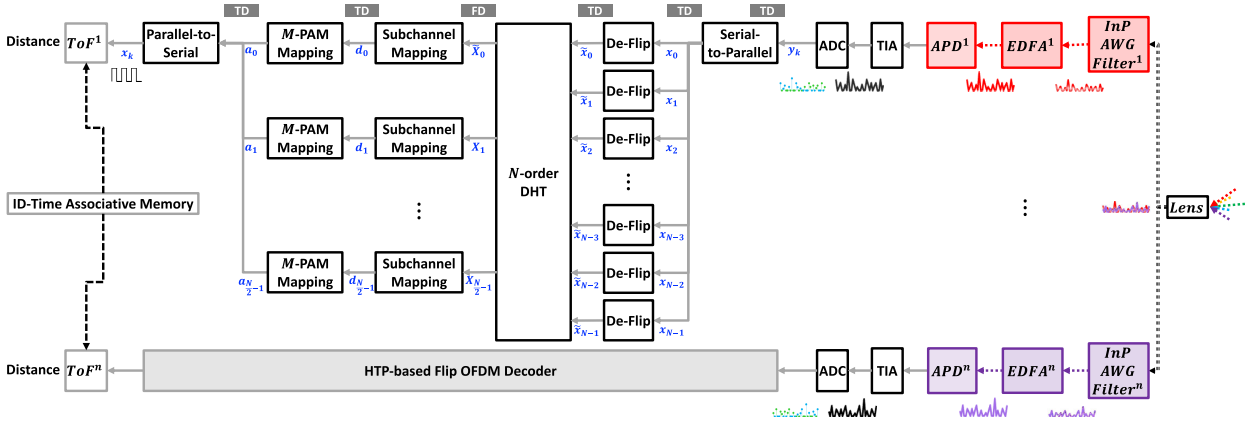

FIGURE 3. Signal processing sequences of the DHT-based flip-OFDM decoder at each receiving carrier.

emission limit (AEL). To address this issue, precoding techniques have been proposed for moderate PAPR reduction gain with small computational complexity, of which the DHT-based flip-OFDM has superior PAPR performance [21].

1) The input data consists of randomly generated 128-bit device identifiers and 128-bit angle identifiers, which are encrypted using AES-128 [12].
2) The transmitter stores the identifiers and compares them with the received data.
3) To increase the data rate, the serially incoming 128-bit encrypted data stream is split into $\frac{N}{2}$ parallel substreams d_i [12].
4) Modulation is performed with $\frac{N}{2}$ parallel substreams using M-pulse amplitude modulation. Each k bit ($k = \log_2 M$) is mapped to the signal constellation set in the TD [12]

$$a_n = A_m d_i \tag{1}$$

where $A_m = 2m - 1 - M$, $m = 1, 2, \ldots, M$.

5) TD symbols X_k are mapped to the even subchannels of N-length FD signals

$$X_n + = \begin{cases} \tilde{X}_k, & n = 2k \\ 0, & otherwise \end{cases} \tag{2}$$

6) FD symbols are fed to N-order IDHT to multiplex the orthogonal subchannels, which result in a TD signal [21]

$$\tilde{x}_n = \frac{1}{\sqrt{N}} \sum_{n=0}^{n-1} X_n \left[cas\left(\frac{2\pi kn}{N}\right)\right] \tag{3}$$

where $n = 0, 1, \ldots, N-1$, n represents FD OOFDMA symbol while $\tilde{x}$ indicates TD output symbol and

$$cas\left(\frac{\pi kn}{N}\right) = cos\left(\frac{\pi kn}{N}\right) + sin\left(\frac{\pi kn}{N}\right) \tag{4}$$

is Hartley kernel.

7) The output from IDHT is sent to the flip operation to generate symbols. The y_k is further decomposed into y_k^+ and y_k^-

$$y_k^+ = \begin{cases} \tilde{x}_n, & \tilde{x}_n > 0 \\ 0, & otherwise \end{cases} \tag{5}$$

$$y_k^- = \begin{cases} \tilde{x}_n, & \tilde{x}_n < 0 \\ 0, & otherwise \end{cases} \tag{6}$$

8) The positive part y_k^+ uses the original position for transmission while the flipped part y_k^- is delayed, and both parts are multiplexed [21]

$$\bar{x}_k = \begin{cases} y_n^+, & 0 \le k \le \dfrac{N}{2} - 1 \\ -y_{k-\frac{N}{2}}^-, & \dfrac{N}{2} \le k \le N - 1 \end{cases} \tag{7}$$

9) N parallel substreams are merged into a serial stream.

The generated OOFDMA signals, as shown in Figure. 1, are connected to 128 laser diodes and external optical modulators (EOMs) with different wavelengths to produce transmit signals with different wavelengths. The outputs of the EOMs are transmitted in the specified direction. This allows multiple laser pulse streams with different wavelengths for the same device and angle identifiers data to be simultaneously transmitted toward different target points. The distance is measured by utilizing the flight time of the pulse stream.

C. ARCHITECTURAL DESIGN AND EXPERIMENTAL IMPLEMENTATION OF THE PROTOTYPE

This study designed a prototype LiDAR to validate the feasibility of the proposed concept. Experimental implementation of the prototype is carried out to validate the feasibility and evaluate the performance of the proposed LiDAR system, as shown in Figure 4. The proposed system consists of commercial off-the-shelf (COTS) products. These include a triple laser source, three high-speed photodetector modules, a four-channel high-speed digitizer, and MATLAB software running on a Windows operating system.

The prototype utilizes a coded laser pulse stream to identify the location and determine the distance to an object. The transmitter, running in MATLAB generates an eight-bit stream comprising a five-bit identification number and a three-bit cyclic redundancy check (CRC) checksum from the most significant bit (MSB) to the least significant bit (LSB). The identification numbers represent the location in each bearing direction. The CRC-3 checksum is an error-detecting code for detecting accidental changes and validating the received bit stream. The power of the laser pulse emitted in the steering direction is equal to or similar to the MPE of class 1 laser products. The four laser pulse stream is coded using the OOFDMA technique to generate a bit stream orthogonal to the other, as shown in Figure 5e and Figure 6e. The OOFDMA encoder saves coded laser pulse stream information when the leading laser pulse is emitted to calculate the time of flight.

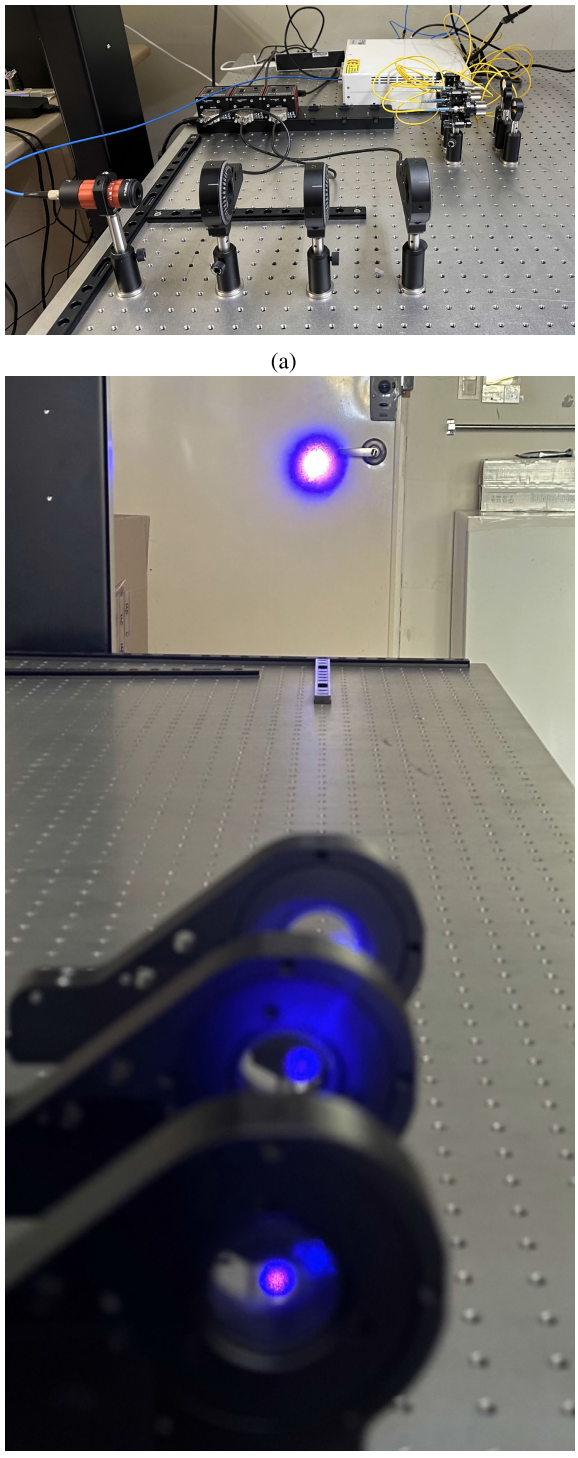

(a)

(b)

FIGURE 4. Experimental implementation of the prototype LiDAR. (a) The entire prototype LiDAR included a triple laser source, three high-speed photodetector modules, and a four-channel high-speed digitizer; (b) Three laser pulse streams are transmitted at different directions according to their wavelengths.

The generated OOFDMA, signals are fed to three laser diodes with different wavelengths in TripleX-WSLS by

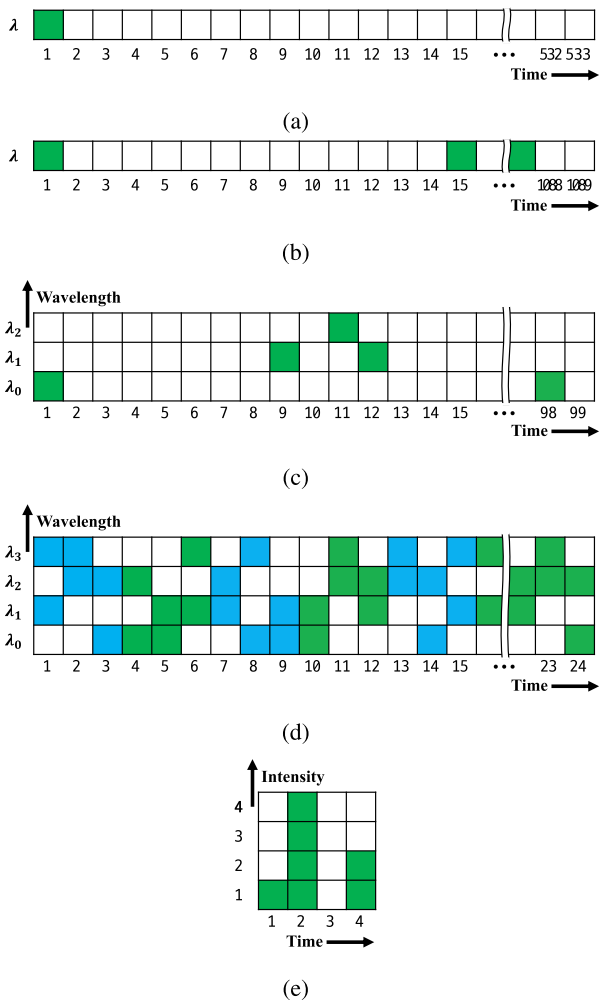

FIGURE 5. Streams encoded according to the codes used by the method of five LiDARs. (a) Single pulse scanning LiDAR uses single pulse only as described in Section IV-A1; (b) Sequential transmitting LiDAR with 1D unipolar optical coded pulse stream uses asynchronous prime sequence code with one wavelength and 121 chips as described in Section IV-A2; (c) Concurrently transmitting LiDAR with 2D unipolar optical coded pulse stream uses carrier-hopping prime codes with three wavelengths and 11 chips as described in Section IV-A3; (d) Concurrently transmitting LiDAR with 2D bipolar optical coded pulse stream uses CIK-based prime permuted code with three wavelengths and 6 chips as described in Section IV-A4; (e) Concurrently transmitting based LiDAR with OOFDMA coded pulse stream uses DHT-based flip-OFDM with one wavelength, 2 subcarriers, and 4 chips as described in Section III.

analog modulation to produce transmission signals with different wavelengths. The TripleX-WSLS from the Wavespectrum Laser Group was chosen because it provides a triple-RGB fiber-coupled white laser source. The red (638nm), green (520nm), and blue (450nm) lasers were integrated into a single fiber to provide the optimal white laser. It consisted of the laser diode (LD), the LD driver, and a thermoelectric (TE) cooling system. Each wavelength was independently controlled by analog modulation. Three optical laser pulse streams are transmitted in three directions according to their wavelengths.

Three receivers are equipped with their own lens that receives the reflected pulse streams, which are then converted into a photocurrent using a high-speed photodetector. The resulting photocurrent of the photodetector is preamplified and converted into a voltage signal by a trans-impedance amplifier (TIA). We used three high-speed photodetectors, the PD1000-VIS from QUBIG, which can operate at frequency up to 1 GHz with a gain of 16 kV A^{-1}. The photodetectors are a high-speed Si PIN photodiode designed to detect visible to near-infrared light with an optimum spectral range of 320 to 1000 nm. The amplified photodetectors have an integrated low-noise TIA which provides a fixed gain resulting in a high signal-to-noise ratio (SNR).

The voltage signals are routed directly to a four-channel high-speed analog-to-digital converter (ADC). We chose an Express CompuScope PCIe Gen3 digitizer CSE161G4 from GaGe RazorMax. This digitizer has four 16-bit channels at 1 GS s^{-1} and 600 MHz bandwidth, with PCIe data streaming rates of up to 5.2 GB s^{-1}. After completing the conversion, the receiving signal processor saves the arrival time and the digitized result to the memory queue. The receiver detects the matched OOFDMA pulse stream using an autocorrelation function from the memory queue. The digitized result is converted into an eight-bit stream in the decoded process. The receiver generates the CRC using a three-bit CRC algorithm that employs a five-bit identification number and compares this CRC with that included in the eight-bit stream. If the two CRCs match, the receiver uses the identification number to identify the time of pulse emission and then calculates the time-of-flight and the distance between the LiDAR and the object. A point cloud image is formed when these processes are conducted for the entire set.

IV. PERFORMANCE EVALUATION

A. OPERATIONAL CHARACTERISTICS OF LiDARs USED FOR COMPARISON

To compare the performance of LiDARs, the prototype was tested in five different modes. Although all LiDARs have the same laser wavelength and pulse width, they differ in encoding method and the pulse stream. The length, pulse count, and pulse position in the pulse stream depend on the pulse coding method employed by the LiDAR instrument. As a result, it determines the time and power required for sending and receiving the pulse stream to measure a point. The image resolution and frame refresh rate depend on the transmission time, while the maximum measurement distance depends on the pulse power. We present the behavioral characteristics of four different LiDAR systems to evaluate the performance against the proposed LiDAR, and the detailed operational parameters are presented in Table 1.

1) SINGLE PULSE SCANNING LiDAR

Pulse LiDAR uses a single laser pulse for a single measurement point [7]. Since the same pulse is used for all measurement points, the discrimination of measurement points from the received pulse is impossible. The time required to measure a single point is longer when it takes

TABLE 1. Characteristics of five LiDARs.

Item		Pulsed LiDAR	Sequential firing LiDAR	Unipolar concurrent firing LiDAR	Bipolar concurrent firing LiDAR	OOFDMA concurrent firing LiDAR (Proposed)
Beam steering mechanism		Body rotation	MEMS mirror	Body rotation	Body rotation	Body rotation
Rotation per second		10	10	10	10	10
Lateral angular resolution		0.191 88°	0.3149°	0.0036°	0.002 16°	0.0018°
Firing cycle time		2.665 µs	6.1 µs	1 µs	0.6 µs	0.5 µs
Dwell time		53.3 µs	781.25 µs	1 µs	0.6 µs	0.5 µs
Field-of-View	Azimuth	360°	40°	360°	360°	360°
	Elevation	40°	40°	40°	40°	40°
Laser beam	Firing mechanism	903 nm	903 nm	903 nm	903 nm	903 nm
	Wavelength	903 nm	903 nm	903 nm	903 nm	903 nm
	Channel	128	128	128	128	128
Spreading method	Coding scheme	N/A	Asynchronous prime sequence code	Carrier-hopping prime code	Code-inversion keying prime permuted code	Discrete Hartely transform based flip-OFDM
	Factor	N/A	Weight 11, length 121	Weight 3, length 11	Weight 3, length 4	4-PAM, 2 subcarrier
	Number of wavelength	1	1	3	4	1
	Line code	N/A	Unipolar NRZ	Unipolar NRZ	Bipolar NRZ	PAM
Pulse stream	Length	N/A	9-bit	9-bit	8-bit	8-bit
	Format	N/A	1-bit SoF, 5-bit ID, 3-bit CRC	1-bit SoF, 5-bit ID, 3-bit CRC	5-bit ID, 3-bit CRC	5-bit ID, 3-bit CRC
	Transmitting method	8 channel at once, 16 transmitting groups	One chip by one chip in sequentially	All channels in concurrent, All wavelengths in concurrent, One chip by one chip in sequentially	All channels in concurrent, All wavelengths in concurrent, One chip by one chip in sequentially	All channels in concurrent, All wavelengths in concurrent, One chip by one chip in sequentially
	Number of time bin	1	1089	99	24	4
	Number of pulse	1	99	27	48	4
	Transmitting time	5 ns	5445 ns	495 ns	120 ns	20 ns
	Example code	Figure 5(a)	Figure 5(b)	Figure 5(c)	Figure 5(d)	Figure 5(e)
	Example waveform	Figure 6(a)	Figure 6(b)	Figure 6(c)	Figure 6(d)	Figure 6(e)
Relative cost and complexity	Optics	Very low	Low	Medium	High	High
	Electronics	Low	Very Low	Low	Medium	High
	Algorithm	Very low	Low	Low	Medium	High

the laser pulse to travel the maximum measurement distance. This results in the longest time of any comparable LiDAR. The MPE is achieved in a single pulse, which makes it the most powerful of all the LIDARs. The laser pulse utilized in this LiDAR is presented in Figure 5a and Figure 6a.

2) SEQUENTIAL TRANSMITTING LiDAR WITH 1D UNIPOLAR OPTICAL CODED PULSE STREAM

This LiDAR uses unipolar direct sequence optical code division multiple access (DS-OCDMA) to incorporate target direction information into its laser pulses [9]. With unipolar coding, each symbol is represented by a single pulse within a chip sequence, with the pulse position indicating the symbol. The length of the chip sequence is proportional to the square of a prime number. It can therefore exceed the cardinality, resulting in longer transmission times. The first laser pulse marks the position of the first chip in the pulse detection frame. The number of additional laser pulses increases the accuracy and precision of pulse detection. There is no need for idle listening time because the laser pulse stream carries the DS-OCDMA-coded directional information. The laser

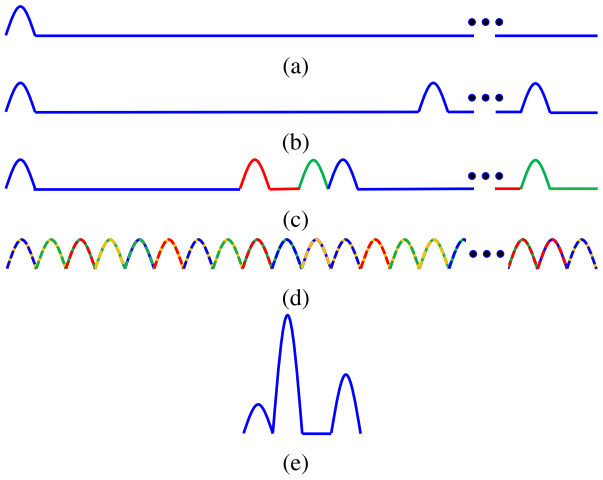

FIGURE 6. Examples of waveforms emitted by five LiDARs. (a) Single pulse scanning LiDAR emits single laser pulse at the beginning of each frame cycle as described in Section IV-A1; (b) Sequential transmitting LiDAR with 1D unipolar optical coded pulse stream emits one laser pulse with one wavelength as described in Section IV-A2; (c) Concurrently transmitting LiDAR with 2D unipolar optical coded pulse stream emits three laser pulses in three different wavelength as described in Section IV-A3; (d) Concurrently transmitting LiDAR with 2D bipolar optical coded pulse stream emits two laser pulse concurrently with two of four different wavelength as described in Section IV-A4; (e) Concurrently transmitting based LiDAR with OOFDMA coded pulse stream emits single laser in one wavelength but different amplitude pulse as described in Section III.

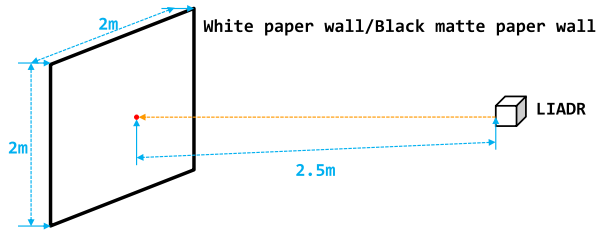

FIGURE 7. Experimental environment.

pulse stream utilized in this LiDAR is presented in Figure 5b and Figure 6b.

3) CONCURRENTLY TRANSMITTING LiDAR WITH 2D UNIPOLAR OPTICAL CODED PULSE STREAM

This LiDAR uses 2D OCDMA modulation with wavelength-hopping time-spread codes to allow simultaneous transmission [16], [17]. For each source, three LDs with different wavelengths are used to generate coded laser pulses. The 2D unipolar optical coding technique can decode the embedded target identification's direction based on the laser pulse's chip position at each wavelength. The transmission time is reduced to a ratio based on the square root of a prime number. Although using multiple wavelengths reduces the transmission time, the same number of laser pulses is required as the total number of wavelengths. The laser pulse stream utilized in this LiDAR is presented in Figure 5c and Figure 6c.

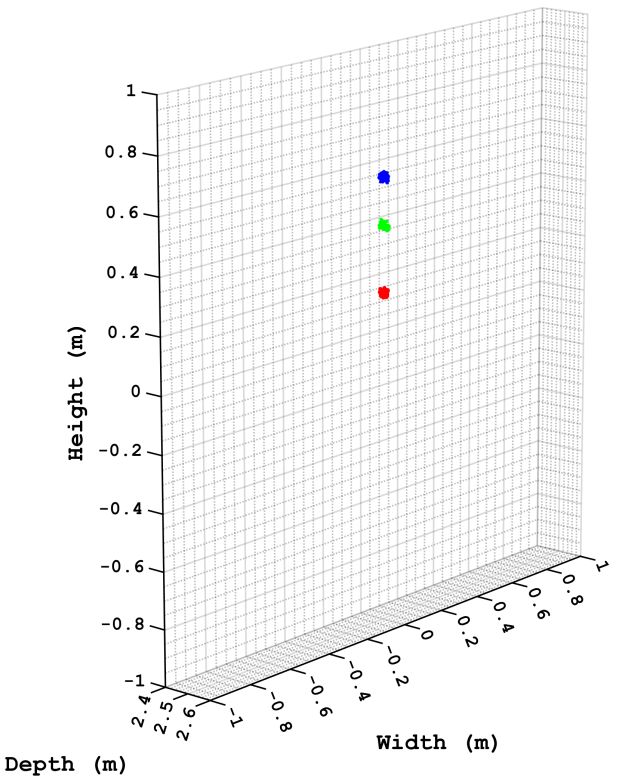

FIGURE 8. Distance measurement of paper wall place at distance of 2.5 m in front of proposed LiDAR.

4) CONCURRENTLY TRANSMITTING LiDAR WITH 2D BIPOLAR OPTICAL CODED PULSE STREAM

This LiDAR uses a 2D prime-permuted code with Walsh codes for wavelength hopping and bipolar Barker sequences for time spreading [27]. This code shortens the long chip sequence required for the simultaneous transmission of the unipolar optical codes of the LiDAR and removes the start of the pulse stream indicator. On-off keying (OOK) modulation is used, where each user transmits a unipolar codeword corresponding to the address codeword of the intended receiver for a data bit ''1''. Prime permuted codes support code inversion keying (CIK). The ''0'' data bits in CIK are transmitted using wavelength-conjugate code words and OOK. Multiple LDs of different wavelengths per channel are combined with a coupler to ensure that the emitted lasers point in the same direction toward the target. The laser pulse stream utilized in this LiDAR is presented in Figure 5d and Figure 6d.

B. DISTANCE MEASUREMENT OF PAPER WALLS

Performance was assessed by measuring distance and intensity with a 2 m × 2 m paper wall placed at a distance of 2.5 m in front of the prototype. Figure 7 shows the configured environment for the experiments, and Figure 8 shows the distance measured by the proposed LiDAR. The distance measurement of the proposed LiDAR was carried out using

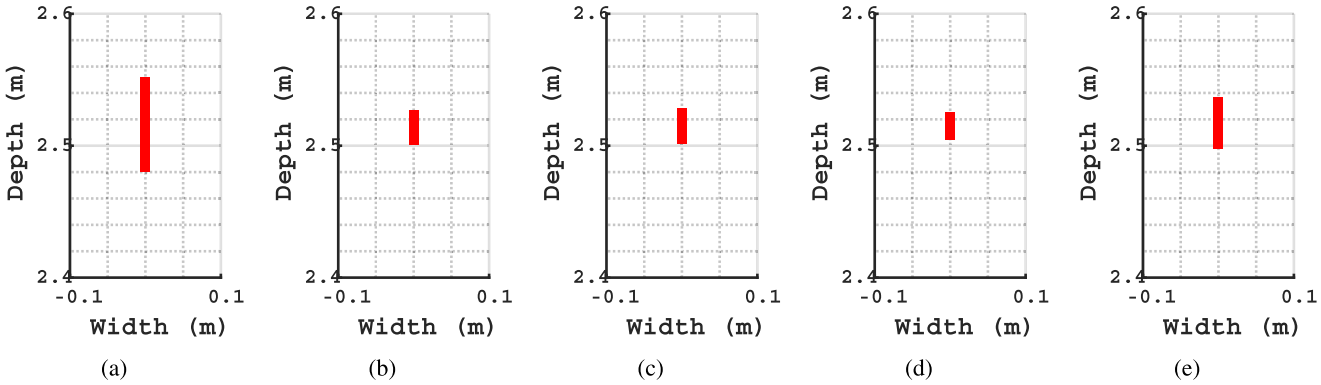

FIGURE 9. The distance was measured 1000 times using a prototype LiDAR on a white paper wall. Five different modes were used. (a) Single pulse scanning LiDAR as described in Section IV-A1; (b) Sequential transmitting LiDAR with 1D unipolar optical coded pulse stream as described in Section IV-A2; (c) Concurrently transmitting LiDAR with 2D unipolar optical coded pulse stream as described in Section IV-A3; (d) Concurrently transmitting LiDAR with 2D bipolar optical coded pulse stream as described in Section IV-A4; (e) Concurrently transmitting based LiDAR with OOFDMA coded pulse stream as described in Section III.

the operation of the LiDAR described in Section III-A, Section III-B and Section III-C.

The analog signal, encoded using OOFDMA, served as the input to the prototype TripleX-WSLS. This laser module produced an optical signal, which was transmitted in different directions based on their respective wavelengths, resulting in a straight-line measurement on the paper wall. The measurement results of the three laser pulse streams are shown in Figure 8. The distances between the three laser pulses were measured as time-of-flight and displayed as point clouds.

C. ACCURACY AND PRECISION

We tested the proposed LiDAR prototype in five modes to evaluate the distance accuracy and precision under different operating conditions, as presented in Table 1. Using white paper placed 2.5 m from the LiDAR, 1000 times measurements were obtained, as shown in Figure 9. The accuracy and precision of the position were measured for the five LiDARs according to the standards of the American Society for Photogrammetry and Remote Sensing (ASPRS) [28]. The distance measurement results vary for different LiDARs, and the line becomes longer as the error increases. Pulsed LiDAR, which uses only one pulse, has the largest error and the smallest number of pulses, as shown in Figure 9(a). Sequential firing LiDAR in Figure 9(b), on the other hand, uses the largest number of pulses and has the smallest error. The unipolar concurrent firing LiDAR in Figure 9(c) and the bipolar concurrent firing LiDAR in Figure 9(d) use fewer pulses than the sequential firing LiDAR, but their range errors are similar. The range error decreases as the number of measurement pulses is increased, but once the number exceeds a certain threshold, the error levels remain constant. The range error decreases as the number of measurement pulses is increased. The increased number of pulses also leads to longer pulse transmission time, resulting in longer measurement and computation times. The method proposed in this study in Figure 9(e) uses OOFDMA, and four pulses for one location, results in the second shortest pulse transmission time among the five LiDARs. However, the method measures the distance with more than twice the accuracy of the single-pulse method. Experimental results for the RSSI, accuracy, and precision of the distance are summarized in Table 2 for better presentation.

TABLE 2. Measured RSSI, accuracy, and precision of five LiDARs.

Item	Single Pulsed LiDAR	Sequential firing LiDAR	Unipolar concurrent firing LiDAR	Bipolar concurrent firing LiDAR	OOFDMA concurrent firing LiDAR (Proposed)
RSSI at 1 m	74 605	41 977	2 844 926	800 507	1 197 647
Accuracy (μm)	47.35	29.226	29.577	29.17	29.167
Precision (μm)	19.121	2.839	3.683	2.763	2.761
Figure	9(a)	9(b)	9(c)	9(d)	9(e)

D. MAXIMUM DISTANCE

Distance and intensity were measured every 0.5 m to determine the system's maximum range. This measurement was done by alternating between a 2 m × 2 m black matte paper wall and a white paper wall. The reflectance of the white paper wall was 90%, and that of the black matter paper wall was 10%. The measured powers in 0.5 m increments from 1 m to 10 m, as shown in Figure. 10. Experiments involve various scanning schemes for the LiDAR, including a single pulse LiDAR and four pulse stream LiDARs working together. This figure shows how the received power correlates to the measured distance. In the case of an extended Lambertian target, the received signal strength is directly proportional to the transmitted power and inversely proportional to the square of the distance. The pulse stream LiDAR outperformed the single pulse LiDAR in all measured distances and for all wall colors.

After the pulse was reflected from the target, the received signal strength was inversely proportional to the square of the distance to the destination. A strong signal was received

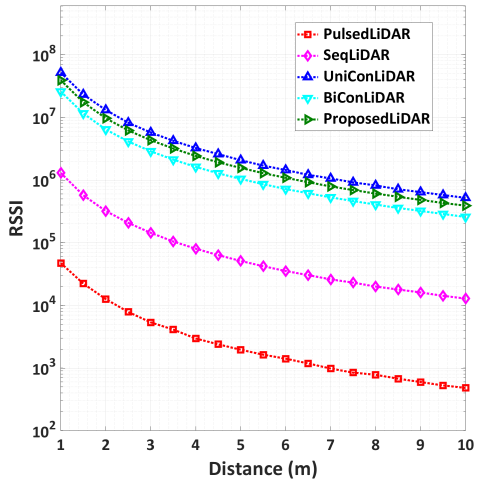

(a)

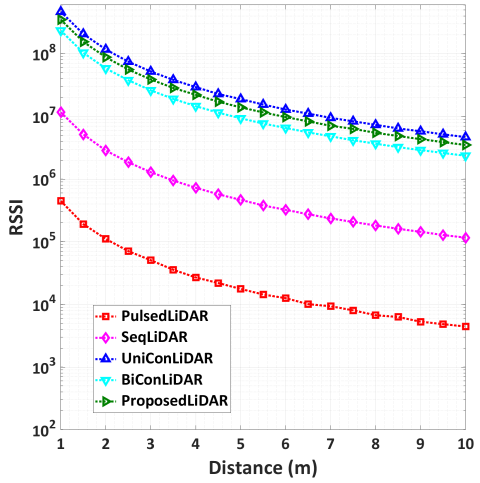

(b)

FIGURE 10. Measured intensity of the five LiDARs from 1 m to 10 m (a) Black matte paper wall; (b) White paper wall.

when the distance to the target was close, and a weak signal was received as the distance was increased. For this reason, when a large SNR was used, the received signal was clearly distinguished from noise, and the false alarm rate was very low; however, the measurement distance was shortened due to the need for a high received signal strength. In the case of using low SNR, the false alarm became high because the received signal is difficult to distinguish from noise, but the low received signal strength was required to obtain maximum range. In the case of LiDAR or radar, a large SNR is preferred because a low false alarm rate is important, and a high received signal strength is used. Each of the received signals was difficult to distinguish from noise, but when multiple pulses were used, it was possible to determine whether they had the same pattern as the transmitted signal by analyzing the pattern. Even if the power of a single pulse is distributed and transmitted, the transmission signal can be detected using a low SNR, so it is possible to measure a similar or distant target compared to the method using a single pulse.

TABLE 3. Simulated maximum distance of five LiDARs.

Item	Single Pulsed LiDAR	Sequential firing LiDAR	Unipolar concurrent firing LiDAR	Bipolar concurrent firing LiDAR	OOFDMA concurrent firing LiDAR (Proposed)
Black matte paper	78 m	92 m	131 m	93 m	139 m
White paper	238 m	278 m	395 m	277 m	417 m

The detection threshold determines the maximum distance the LiDAR can measure. Noise can have any value and can reach the detection threshold. In addition, the amplitude value is the result of contributions from both the noise and the reflectivity of the target, if present. Lowering the detection threshold increases the probability of detection and the probability of exceeding the noise threshold, resulting in an increased number of false alarms. The probability of a false alarm (P_{FA}) affects the correctness of the return laser pulse detection and the measured distance. Unlike pulse-stream LiDARs, which rely on a pulse stream and eliminate spurious pulses through multiple detection steps and CRC checksums, single-pulse LiDARs rely on single pulse detection and signal processing during the reception process. Due to the discrepancy between the two LiDARs, the single pulsed LiDAR necessitated an extremely low P_{FA} and employed a high ratio of threshold-to-noise (TNR). However, the pulse stream LiDARs rely on a high P_{FA} and low TNR.

We simulated the received power based on the measured power and the relationship between the received power, measured distance, and target surface reflectivity. Simulations are carried out using Synopsys RSoft OptSim [15], [29] optical simulation software and MathWorks MATLAB R2023b [15], [16], [30]. We included the optical characteristics related to the reflection, lens, laser transmission, and reception, as well as the encoding and decoding, signal processing, intensity calculation, and distance calculation tasks [12], [15], [24]. Table 3 and Figure 11 show the simulated maximum detectable distance using the received signal strength when measuring the white paper wall and black matte paper wall with five LiDAR scanners.

Simulation results demonstrate that the proposed LiDAR can effectively detect obstacles and has significant potential for practical applications. For the pulse stream LiDARs, the intensity was calculated by summing the peak amplitudes of received pulses for the same target. Compared to the single pulse LiDAR, the pulse stream LiDAR had a several times higher intensity value. The sequential firing LiDAR scanner and the concurrent firing LiDAR scanner could detect signals that were not clearly distinguished from noise by using multiple reflected laser pulses. Compared to the black matte paper wall, the white paper wall had higher reflectivity, so all five LiDARs could equally measure a longer distance with the white paper wall. The laser output of the sequentially transmitted LiDAR scanner was lower than that of the single pulsed LiDAR, but it was possible to detect reflected waves

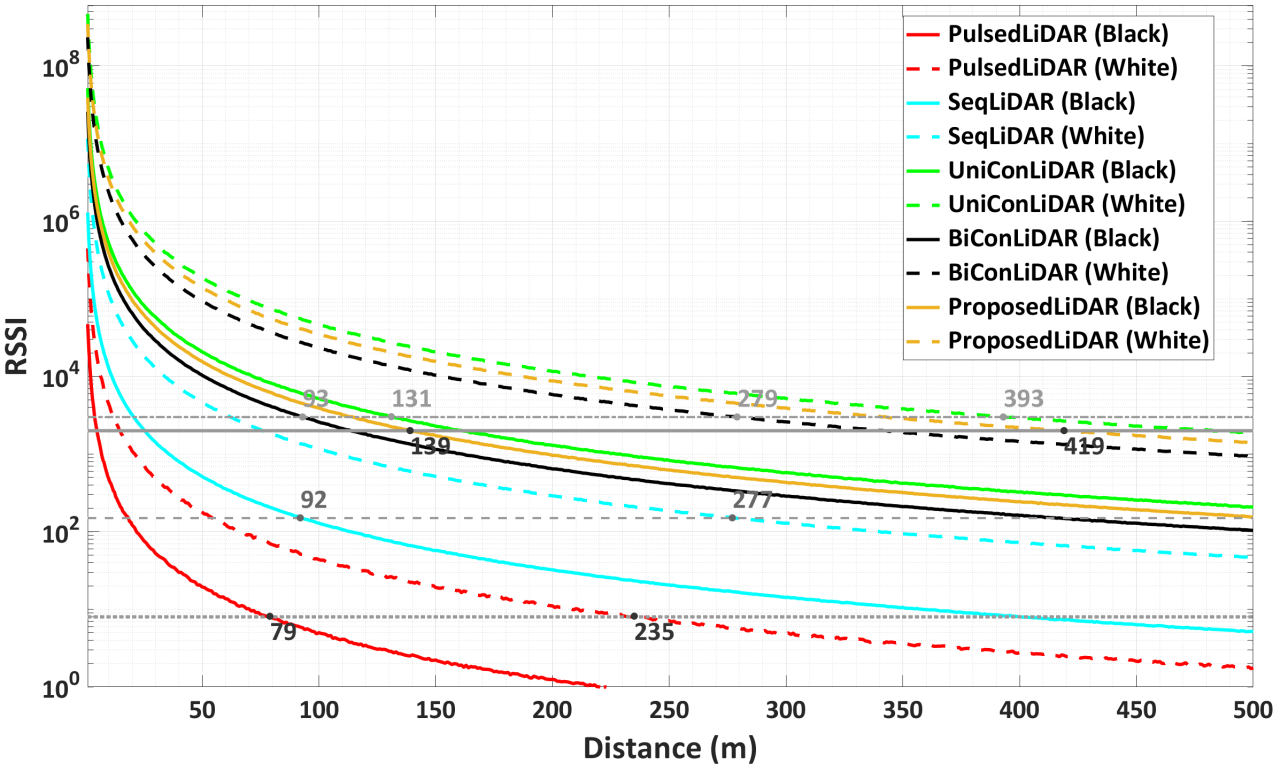

FIGURE 11. Max Distance.

over a longer distance by using multiple reflected laser waves.

V. CONCLUSION

The future of transportation is foreseen to transform by integrating a vast range of terrestrial and aerial modes of conveyance. Ensuring the safety and efficiency of these transportation systems is of utmost importance, and the significance of vision-based sensors, specifically LiDAR, should not be underestimated. Despite its preliminary cost and obstacles, LiDAR technology has emerged as an indispensable perception sensor for autonomous vehicles. Its precise 3D spatial scanning, high lateral angular resolution, and robust object detection capabilities make LiDAR a unique sensor for vehicles. However, it is significantly important to address challenges like lateral angular resolution and frame rate trade-offs and mitigate interference issues that arise when multiple LiDARs operate simultaneously. With these challenges overcome, LiDAR is positioned to play a crucial role in bringing about a new age of transportation systems that are safe, efficient, and reliable.

The proposed LiDAR system, which leverages OOFDMA and advanced coding techniques, is a promising solution to resolve mutual interference issues among multiple LiDARs. Generating distinctive pulse streams and using encrypted identifiers to specify transmission directions, this technology ensures accurate measurements while reducing latency for distance calculations. Simulations show the potential of this LiDAR system in effectively detecting obstacles and opening doors to practical applications. Pulse stream LiDARs have demonstrated superiority over single-pulse LiDARs in scenarios with low reflectivity surfaces, delivering optimized range and accuracy. OOFDMA coding represents a promising technology for increasing the robustness and versatility of LiDAR-based perception systems as LiDAR technology continues to evolve. This innovation will continue to contribute to advancements in future mobility solutions.

ACKNOWLEDGMENT

(Gunzung Kim and Imran Ashraf are co-first authors.)

REFERENCES

[1] S. Royo and M. Ballesta-Garcia, "An overview of LiDAR imaging systems for autonomous vehicles," *Appl. Sci.*, vol. 9, no. 19, p. 4093, Sep. 2019.

[2] Y. Cao, C. Xiao, B. Cyr, Y. Zhou, W. Park, S. Rampazzi, Q. A. Chen, K. Fu, and Z. M. Mao, "Adversarial sensor attack on LiDAR-based perception in autonomous driving," in *Proc. ACM SIGSAC Conf. Comput. Commun. Secur.*, Nov. 2019, pp. 2267–2281.

[3] R. Roriz, J. Cabral, and T. Gomes, "Automotive LiDAR technology: A survey," *IEEE Trans. Intell. Transp. Syst.*, vol. 23, no. 7, pp. 6282–6297, Jul. 2022.

[4] Z. Dai, A. Wolf, P.-P. Ley, T. Glück, M. C. Sundermeier, and R. Lachmayer, "Requirements for automotive LiDAR systems," *Sensors*, vol. 22, no. 19, p. 7532, Oct. 2022.

[5] I. Ashraf, S. Hur, and Y. Park, "An investigation of interpolation techniques to generate 2D intensity image from LiDAR data," *IEEE Access*, vol. 5, pp. 8250–8260, 2017.

[6] P. F. McManamon, *Field Guide to LiDAR* (Field Guide), vol. FG36. Bellingham, WA, USA: International Society for Optics and Photonics, 2015.

[7] *VLS-128 User Manual*, Velodyne LiDAR Inc., San Jose, CA, USA, 2018.

[8] *Operating Instructions for Laser Measurement Sensors of the LMS5xx Product Family*, SICK AG, Waldkirch, Germany, 2015.
[9] G. Kim and Y. Park, "LiDAR pulse coding for high resolution range imaging at improved refresh rate," *Opt. Exp.*, vol. 24, no. 21, p. 23810, 2016.
[10] F.-W. Lo, G.-C. Yang, W.-Y. Lin, I. Glesk, and W. C. Kwong, "2-D optical-CDMA modulation with hard-limiting for automotive time-of-flight LiDAR," *IEEE Photon. J.*, vol. 13, no. 6, pp. 1–11, Dec. 2021.
[11] G. Lee, J. K. Park, and J. T. Kim, "OCDMA codeword switching technique to avoid interference of time-of-flight LiDAR system for autonomous vehicles," *IEEE Sensors J.*, vol. 23, no. 3, pp. 3090–3102, Feb. 2023.
[12] Z. Ghassemlooy, W. Popoola, and S. Rajbhandari, *Optical Wireless Communications: System and Channel Modelling With MATLAB*. Boca Raton, FL, USA: CRC Press, 2019.
[13] C. Goursaud-Brugeaud, A. Julien-Vergonjanne, and J.-P. Cances, "Prime code efficiency in DS-OCDMA systems using parallel interference cancellation," *J. Commun.*, vol. 2, no. 3, pp. 51–57, May 2007.
[14] Y. Liang, J. Huang, M. Ren, B. Feng, X. Chen, E. Wu, G. Wu, and H. Zeng, "1550-nm time-of-flight ranging system employing laser with multiple repetition rates for reducing the range ambiguity," *Opt. Exp.*, vol. 22, no. 4, p. 4662, 2014.
[15] G. Kim and Y. Park, "Independent biaxial scanning light detection and ranging system based on coded laser pulses without idle listening time," *Sensors*, vol. 18, no. 9, p. 2943, Sep. 2018.
[16] G. Kim, I. Ashraf, J. Eom, and Y. Park, "Concurrent firing light detection and ranging system for autonomous vehicles," *Remote Sens.*, vol. 13, no. 9, p. 1767, May 2021.
[17] G. Kim, J. Eom, and Y. Park, "Alien pulse rejection in concurrent firing LiDAR," *Remote Sens.*, vol. 14, no. 5, p. 1129, Feb. 2022.
[18] G. Kim and Y. Park, "Suitable combination of direct intensity modulation and spreading sequence for LiDAR with pulse coding," *Sensors*, vol. 18, no. 12, p. 4201, Nov. 2018.
[19] J. Dang and Z. Zhang, "Comparison of optical OFDM-IDMA and optical OFDMA for uplink visible light communications," in *Proc. Int. Conf. Wireless Commun. Signal Process. (WCSP)*, Oct. 2012, pp. 1–6.
[20] Z. Muhammad, H. Mahmood, A. Ahmed, and N. A. Saqib, "Selective HARQ transceiver design for OFDM system," *IEEE Commun. Lett.*, vol. 17, no. 12, pp. 2229–2232, Dec. 2013.
[21] A. W. Azim, "Signal processing techniques for optical wireless communication systems," Ph.D. dissertation, ANS, Grenoble INP, Université Grenoble Alpes (ComUE), 2018.
[22] G. Garcia-Torales, "Risley prisms applications: An overview," *Proc. SPIE*, vol. 12170, pp. 136–146, May 2022.
[23] J. Zhou, Y. Qiao, Z. Cai, and Y. Ji, "An improved scheme for flip-OFDM based on Hartley transform in short-range IM/DD systems," *Opt. Exp.*, vol. 22, no. 17, p. 20748, 2014.
[24] K. Szczerba, P. Westbergh, J. Karout, J. S. Gustavsson, Å. Haglund, M. Karlsson, P. A. Andrekson, E. Agrell, and A. Larsson, "4-PAM for high-speed short-range optical communications," *J. Opt. Commun. Netw.*, vol. 4, no. 11, pp. 885–894, Nov. 2012.
[25] A. Li, *Double-Prism Multi-mode Scanning: Principles and Technology*, vol. 216. Cham, Switzerland: Springer, 2018.
[26] S. Li, J. Cao, Y. Cheng, L. Meng, W. Xia, Q. Hao, and Y. Fang, "Spatially adaptive retina-like sampling method for imaging LiDAR," *IEEE Photon. J.*, vol. 11, no. 3, pp. 1–16, Jun. 2019.
[27] G. Kim, J. Eom, and Y. Park, "2D bipolar optical codes based concurrent transmitting LiDAR with code-inversion keying-based prime-permuted code," *IEEE Access*, vol. 11, pp. 64185–64200, 2023.
[28] D. Smith, Q. Abdullah, D. Maune, and H. Heidemann, "New ASPRS positional accuracy standards for digital geospatial data released," *Photogramm. Eng. Remote Sens.*, vol. 81, pp. 1073–1085, Jan. 2015.
[29] E. Ghillino, E. Virgillito, P. V. Mena, R. Scarmozzino, R. Stoffer, D. Richards, A. Ghiasi, A. Ferrari, M. Cantono, A. Carena, and V. Curri, "The synopsys software environment to design and simulate photonic integrated circuits: A case study for 400G transmission," in *Proc. 20th Int. Conf. Transparent Opt. Netw. (ICTON)*, Jul. 2018, pp. 1–4.
[30] M. T. Sullivan, "Synopsis of Risley prism beam pointer," Lockheed Martin Space Syst., Hanover Street, Palo Alto, CA, USA, Tech. Rep., 2006.

GUNZUNG KIM (Member, IEEE) was born in Daegu, Republic of Korea, in 1972. He received the B.S. and M.S. degrees in computer engineering and the Ph.D. degree in multimedia and communication engineering from Yeungnam University, Republic of Korea, in 1995, 1997, and 2019, respectively. He is currently a Research Professor with Yeungnam University. His research interests include LiDAR, optical communication, and vehicle software.

IMRAN ASHRAF received the M.S. degree in computer science from the Blekinge Institute of Technology, Karlskrona, Sweden, in 2010, and the Ph.D. degree in information and communication engineering from Yeungnam University, Gyeongsan-si, South Korea, in 2018. He was a Postdoctoral Fellow with Yeungnam University, where he is currently an Assistant Professor with the Information and Communication Engineering Department. His research interests include indoor positioning and localization, indoor location-based services in wireless communication, smart sensors (LiDAR) for smart cars, and data mining.

JEONGSOOK EOM was born in Daegu, Republic of Korea, in 1975. She received the B.S. and M.S. degrees in computer engineering from Yeungnam University, Republic of Korea, in 1998 and 2001, respectively, where she is currently pursuing the Ph.D. degree in multimedia and communication engineering. Her research interests include LiDAR, optical communication, and mutual interference between active sensors.

YONGWAN PARK (Member, IEEE) was born in Daegu, Republic of Korea, in 1959. He received the B.E. and M.E. degrees in electrical engineering from Kyungpook University, Daegu, in 1982 and 1984, respectively, and the M.S. and Ph.D. degrees in electrical engineering from the State University of New York at Buffalo, USA, in 1989 and 1992, respectively. He is currently a Professor with Yeungnam University and also the Chairperson of the 5G Forum Convergence Service Committee, Republic of Korea. His current research interests include 5G systems in communication, OFDM, PAPR reduction, and indoor location-based services in wireless communication and smart sensors (LiDAR) for smart cars.